



Effect of the temperatures on structural and optical properties of tin oxide (SnO_x) powder

N.M.A. Hadia^{a,b,*}, S.V. Ryabtsev^b, P.V. Seredin^b, E.P. Domashevskaya^b

^a Department of physics, Faculty of Science, Sohag University, 82524-Sohag, Egypt

^b Voronezh State University, Universitetskaya pl. 1, 394006, Voronezh, Russia

ARTICLE INFO

Article history:

Received 8 November 2008

Received in revised form

18 August 2009

Accepted 18 August 2009

PACS:

61.10.Nz

74.25.Gz

78.30.-j

78.40.Fy

Keywords:

SnO powder

SnO_2

Temperatures

Structural and optical

ABSTRACT

A series of composite SnO_x materials were prepared by SnO powder heating at different temperatures in air for 2 hr. Depending on treatment conditions it was found that SnO, with its tetragonal structure, could transform into the Sn phase or tetragonal SnO and tetragonal SnO_2 . The influence of heating at different temperatures on the properties of SnO_x has been studied. The influences of annealing temperatures in air on the structural and optical properties of SnO_x have been investigated. Correlations between the structural and optical properties of the products were found.

© 2009 Elsevier B.V. All rights reserved.

1. Introduction

Tin oxide is of great technological interest as transparent conducting electrodes, IR reflecting heat mirrors, and SnO/Si solar cell devices with high conversion efficiency [1]. Moreover, SnO_2 -based sensor devices have been used as a prototype for detecting reducing and inflammable gases [2]. Tin oxide thin films have been successfully demonstrated as transparent conductors (TC), optical windows for the solar spectrum, stability resistors, touch-sensitive switches, digital displays, light emitting diodes (LEDs), electrochromic displays (ECDs), etc. [3], mainly due to their outstanding properties.

The consensus of the researchers is that for TC, high transmittance (T%) and relatively low electrical resistivity (ρ) is desirable while for applications such as display devices and LEDs, low electrical resistivity and moderate transmittance are desirable [4]. These applications rely on its itinerant electrons that stem from the ionization of the dopants and enter the conduction band. For ECDs, which hinges on the ability of the material to sustain mixed conduction of ions and electrons, low electrical resistivity is

more desirable than high transmittance [5], additionally it is useful to have some water content in the resultant film [4], which plays key role in inducing electrochromic (EC) effect.

It is noticed from the literature survey that the variety of methods of preparation will lead to the layers having different optical and electrical properties, which evokes critical influence of oxygen vacancies, serving as donor in tin oxide films [5]. In principle physical methods such as sputtering [3], and thermal evaporation [6], lead to weakly non-stoichiometric tin oxide with co-existence of other insulating phases like SnO, resulting into relatively high resistive films. The range of resistivity of as deposited SnO_x films typically varies from $6.6 \times 10^{-3} \Omega \text{cm}$ to $2.5 \times 10^{-3} \Omega \text{cm}$ [3]. On the other hand chemical methods especially spray pyrolysis technique, lead to strongly non-stoichiometric tin oxide films without co-existence of insulating phases, resulting into comparatively low resistive films [7]. The electrical resistivity of as deposited SnO_x films typically varies from $1.45 \times 10^{-3} \Omega \text{cm}$ to $0.45 \times 10^{-3} \Omega \text{cm}$, which is several times less than the films deposited by physical methods. Therefore, it can be concluded that the SnO_x films deposited by spray pyrolysis technique are more susceptible to oxygen deficiencies [8].

We are interested in SnO_x films in connection with the electrochromism. Electrochromic tin oxide films were described recently by Orel et al. [9] and Olivi et al. [10] who prepared their samples by dip-coating and Isidorosson et al. [11] who prepared

* Corresponding author at: Voronezh State University, Universitetskaya pl. 1, 394006, Voronezh, Russia. Tel/fax: +7 0732 208 363.

E-mail address: Nomery_abass@yahoo.com (N.M.A. Hadia).

their samples by sputtering. They emphasize the importance of various properties that SnO_x should exhibit for attaining pronounced electrochromism.

In this investigation, we have employed spray pyrolysis technique for SnO_x thin film deposition and discussed their structural, electrical and optical properties. The deposition has been carried out from aqueous stannic chloride solution, with a postulation that the resultant films may have some water content [11], which would be in turn beneficial for better electrochromic effect. Several experiments on electrochromism in SnO_x thin films are underway and results will be disseminated elsewhere.

SnO_2 is an n-type semiconductor with an optical band gap of about 3.6 eV. SnO_2 crystallizes in the rutile structure D_{4h}^{14} [12]. In rutile SnO_2 , each atom is surrounded by a distorted octahedron of O atoms with all Sn distances equal to 2.05 Å. In comparison with SnO_2 , the structure and physical properties of SnO have not been extensively investigated. The structure of SnO is layered, similar to that of PbO, with tetragonal structure D_{4h}^{14} [12]. In this structure the Sn^{2+} is situated at the apex of a square pyramid with Sn–O distances equal to 2.224 Å and O–Sn–O angles 11.73°. Also, SnO exists in an orthorhombic phase depending on the preparation procedures. The optical band gap is in the range 2.5–3 eV.

The oxidation of tin and in particular the mechanism of the oxidation process from SnO to SnO_2 have been extensively studied using various kinds of preparation techniques [13]. In general, when tin oxide films were deposited on a high temperature substrate by several deposition techniques, since it dissociates in the gaseous SnO and forms oxygen-deficient SnO_x ($x < 2$) films, post-annealing in an O_2 environment should be given. Geurts et al. [14] and Reddy et al. [13] found that the annealed films reach the final oxidation state either through simple oxidation of SnO (direct transition) or through intermediate oxidation states (indirect transition), namely Sn_2O_3 or Sn_3O_4 , depending on the deposition parameters.

According to most previous studies [13], the oxidation of SnO and SnO_2 was carried out without knowledge of the initial oxygen content in as-deposited films and it was reported that the perfect SnO_2 formation could only be attained after above 600 °C annealing in O_2 exposure. Therefore the influences of initial composition, which intimately depend on deposition parameters, on the oxidation process and crystallization from SnO and SnO_2 were not yet systematically clarified as the annealing temperature increased.

Moreover, many extensive investigations of the oxidation state of tin oxide have been carried out using Auger electron spectroscopy (AES), core-level and valence-band (VB) X-ray photoelectron spectroscopy (XPS), ion scattering spectroscopy (ISS), and ultraviolet photoelectron spectroscopy (UPS) [15], but quantitative analysis is complicated by the difficulty of preparing standard samples with an accurately known composition, and the modification of surface composition by an incident electron or ion beam.

Detailed analyses of the VB region led to the distinction between SnO and SnO_2 by UPS and VB XPS, where the presence of the prominent leading peak of a Sn 5s-derived origin for SnO and that of an O 2p-derived structure at the lower binding energy side of the VB in SnO_2 uses the characteristic peak to distinguish the SnO and SnO_2 phases [16]. Recently Themlin et al. [17] and Sanjinjs et al. [18] reported that a sizable chemical shift of 0.7 eV between Sn^{2+} (SnO) and Sn^{4+} (SnO_2) by XPS. In a previous report [19], we also found that the chemical shift between Sn^{2+} and Sn^{4+} occurred as much as 1.0 ± 0.02 eV in XPS analyses and $2\text{--}4 \pm 1$ eV in AES spectra. However, the chemical shift measured from AES spectra was not reliable because main doublet Auger transitions ($M_5 N_{4,5} N_{4,5}, M_4 N_{4,5} N_{4,5}$) in tin oxide were not well resolved.

Ultraviolet photoelectron spectroscopy experiments for surface electronic structure of tin oxide were performed only on single crystal SnO_2 (001) and SnO_2 (110) surfaces using synchrotron light and He I UV sources [20]. Cox et al. [21] found unusual band gap emission at the clean SnO_2 crystal surface after Ar^+ bombardment and Themlin et al. [35] also reported that the tin-derived character of the band gap defect states was found in the perturbed SnO_2 (110) surface by the ion bombardment.

In this present work, we thoroughly examine the oxidation processes of SnO powder heated at different temperatures in air for 2 hr. The variations of the structural properties of SnO_x that have happened through SnO to SnO_2 transformation are investigated. The effects of annealing temperatures on the optical and structural properties of the products are discussed.

2. Experimental details

99.99% pure SnO powders were placed in an alumina boat positioned at the centre of the quartz tube. The temperature of the furnace was rapidly ramped up to 250, 450, 650 and 850 °C and kept for 2 hr. During the process, a constant flow of air was adjusted. The crystal structure of the SnO_x were characterized by X-ray diffraction (XRD) using a DRON 4 utilizing Cu K_α radiation. UV/visible absorption measurements were carried out on the SnO_x using a spectrophotometer (UV-210A, Shimadzu) in the wavelength range between 190 and 900 nm. The IR studies were carried out at room temperature using FIR -spectrometer Vertex 70 (Bruker).

3. Results and discussions

3.1. X-ray diffraction studies

The crystal structure and phase of the powder samples were determined from the XRD patterns. Fig. 1 shows X-ray diffraction (XRD) patterns of the SnO powder heating at different temperatures (250, 450, 650 and 850 °C) for 2 hr in air and SnO_2 powder. All the peaks in Fig. 1(a and b) can be readily indexed as tetragonal SnO (JCPDS, no. 06-0395) with cell parameters $a=3.80$ Å and $c=4.84$ Å. Comparing the XRD spectrum of the standard tetragonal SnO powder (Fig. 1a), the XRD spectrum of SnO powder heated at 450 °C (Fig. 1c) shows a very strong feature of texture structure. Fig. 1c is indexed as (200), (110), (102), (211), (301), (400) for Sn, (101), (110), (002), (200), (112), (211), (103), (220), (004) for SnO and (110), (101), (200),

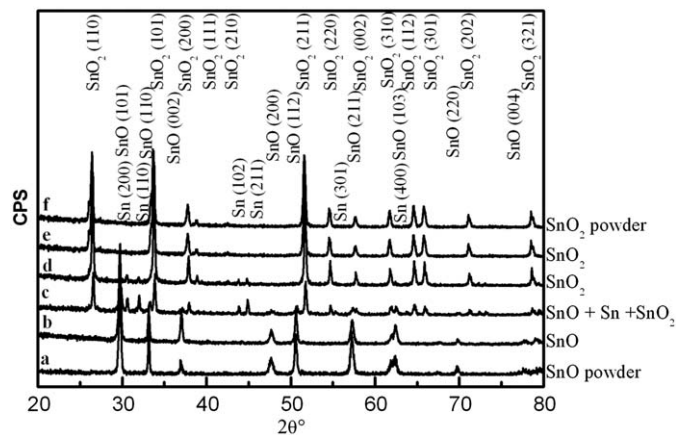


Fig. 1. XRD spectra of source material SnO powders annealing at different temperatures 250, 450, 650 and 850 °C for 2 h in air and SnO_2 powder.

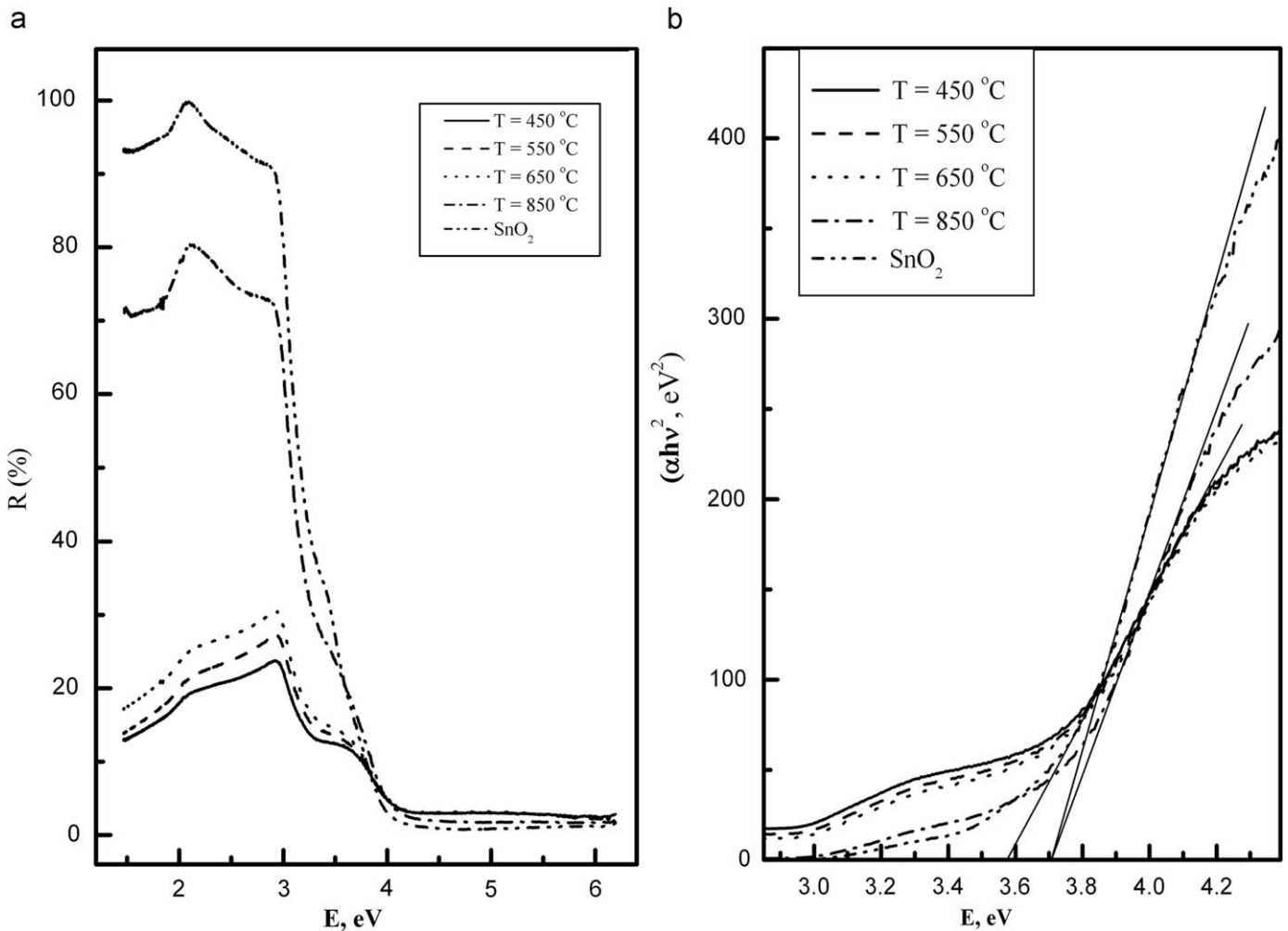


Fig. 2. (a) Spectral variation of reflectance (R) for all the samples SnO annealed at $T=450^\circ\text{C}$, 550°C , 650°C , 850°C for 2 h in air and SnO_2 powder). (b) The variation of $(\alpha hv)^2$ versus $h\nu$ for all the samples, SnO annealed at $T=450^\circ\text{C}$, 550°C , 650°C , 850°C for 2 h in air and SnO_2 powder).

(211), (220), (002), (310), (112), (301), (202), (321) for SnO_2 . Therefore, Sn, SnO and SnO_2 are simultaneously present at the annealing temperature of 450°C , and the intergrowth mechanisms may occur at this thermal oxidizing temperature [22]. Increasing the annealing temperature further to 650°C , the Sn and SnO diffraction peaks disappeared and a complete transformation of SnO to a tetragonal rutile structure SnO_2 powders is observed. The thermal oxidation process of SnO to SnO_2 may be described as follows [23]: due to the existence of oxygen environment, the oxidation begins at the surface of the Sn particles, and SnO and SnO_2 phases are nucleated and formed as dispersed clusters on the surface of the Sn particles. The SnO_2 clusters keep on growing into nanoparticles when the temperature is high enough to allow oxygen to diffuse into the SnO particles. Fig. 1(d, e and f) represent only the characteristic SnO_2 peaks corresponding to (110), (101), (200), (111), (210), (211), (220), (002), (310), (112), (301), (202) and (321) planes and the SnO powder is believed to be perfectly oxidized to SnO_2 . As temperature increases from 650 to 850°C , no changes in positions and intensities of the XRD peaks are found.

From this observation it is proved that the annealing temperature of 450°C is not high enough to form the highest oxidation state of SnO_2 . It was reported in [24] that the annealed of polycrystalline SnO could completely reach pure polycrystalline SnO_2 after post-annealing at temperatures higher than 600°C in an O_2 atmosphere. In consequence, the oxidation from SnO to

SnO_2 intimately depends on the initial content of oxygen and the annealing temperature.

3.2. Optical properties of SnO_x

It is well known that SnO_2 is a degenerate semiconductor with band gap energy (E_g) in the range of 3.4–4.6 eV [25]. This scatter in band gap energy (E_g) values of SnO_2 may be due to wide extent of non-stoichiometry of the deposited layers. The dependency of the band gap energy on the carrier concentration has been explicitly given in the literature [25]. It has been apprehended that band gap energy increases linearly with the increase in carrier concentration to the power $2/3$.

Fig. 2(a and b) shows the reflectance and the variation of $(\alpha hv)^2$ versus $h\nu$ for SnO powder annealed at different temperatures (450 , 550 , 650 and 850°C) and SnO_2 powder. The nature of the plots indicates the existence of direct optical transitions. The band gap (E_g) is determined by extrapolating the straight-line portion of the plot to the energy axis. The intercept on energy axis gives the value of band gap energy E_g for all the samples and the values lie in the range of 3.58–3.73 eV. It is noticed that band gap energy value is minimum (3.58 eV) for SnO samples annealed at 450°C . The samples annealed at 550 and 650°C , have E_g values amongst all other samples, owing to lower carrier concentration. Increasing the annealing temperature to

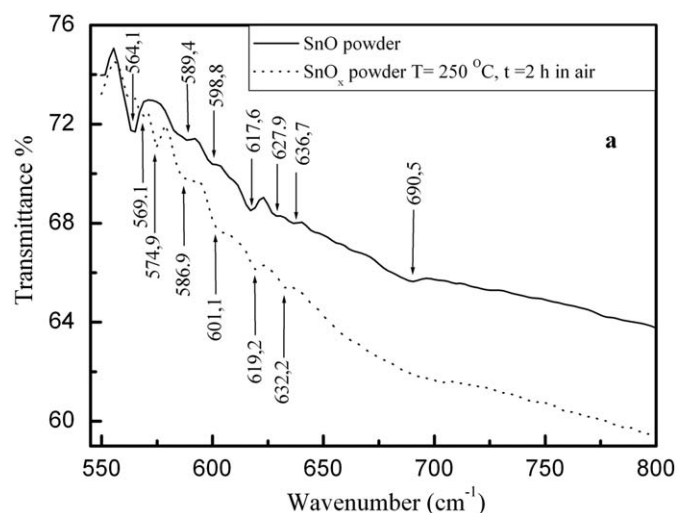


Fig. 3. (a) IR spectra of source material SnO powders annealing at different temperatures 250, 450, 650 and 850 °C for 2 h in air and SnO₂ powder. (b) IR spectra of source material SnO powders annealing at different temperatures 250, 450, 650 and 850 °C for 2 h in air and SnO₂ powder.

Table 1

IR band positions and assignments for SnO powder annealing in air at different temperatures (250, 450, 650 and 850 °C) for 2 h and SnO₂ powder.

ν (cm ⁻¹)	Reference	Fundamental Vibrations ^a
540 [30]; 555.7 [*] ; 558.1 [*] ; 559.5 [*] ; 561 [31]; 562.2 [*] ; 564 [*] ; 565.3 [*] ; 569.7 [*] ; 574.9 [*] ; 579.7 [*] ; 580.1 [*] ; 586.8 [*] ; 596.2 [*] ; 599.6 [*] ; 601.1 [*] ; 604.1 [*] ; 605.5 [*]	[30,31], this work [*]	ν (Sn–O, T)
610 [29]; 617.6 [*] ; 619.2 [*] ; 631.1 [*] ; 632.2 [*] ; 636.7 [*] ; 647.1 [*]	[29], this work [*]	ν (Sn–O)
650 [28]; (665,667) [30]; 668.6 [*] ; 680 [31]; 690 [28]; 690.5 [*] ; 703.7 [*] ; 728.9 [*] ; 742.2 [*] ; 757.1 [*] ; (737; 770) [27]; 774.3 [*]	[28] [30,31], this work [*]	ν (Sn–O) ν (Sn–O–Sn)
	[28], this work [*] [27], this work [*]	ν (Sn–O) ν_{as} (Sn–O–Sn)

^a T: terminal; B: bridged

850 °C, a maximum value of 3.72 eV is attained for SnO₂. The increase in E_g values with increasing annealing temperature may be ascribed to the increase in the carrier concentration. As carrier concentration is higher, absorption of the light by the carriers also increase, leading to higher absorption coefficient (α) in the samples annealed at 850 °C and SnO₂.

The constituents of valance and conduction band in SnO₂ have been described by Munnix and Schmeits [26]. The width of the valance band is about 9 eV, which has been segmented in three different regions resulting from, (i) coupling of Sn s orbitals and O p orbitals, (ii) mingling of O p orbitals with smaller fraction of Sn p orbitals and (iii) mainly O p lone pair orbitals. The Sn s states mainly contribute to the formation of bottom of conduction band and top of conduction band has dominated Sn p character. The

above discussion is clear enough to understand $s \rightarrow p$ direct optical transition in SnO₂.

3.3. IR studies of SnO_x

The IR transmittance spectra of the SnO powder heating at different temperatures (250, 450, 650 and 850 °C) for 2 hr in air and SnO₂ powder in the low frequency range 550–800 cm⁻¹ are shown in Fig. 3. Several bands due to fundamentals, overtones and combinations of OH, Sn–O and Sn–O–Sn entities appear in the 4000–800 cm⁻¹ range. Below 800 cm⁻¹, the cut-off arising from lattice vibrations is occurred.

The results and the proposed attributions are presented in Table 1 and compared with the data published in the literatures [27–31]. The discrepancies concerning are due to several factors: (i) the nature of the sample (monocrystal, powder, colloidal suspension) and the proportion of low-coordination sites [32]; (ii) the stoichiometry of the oxide, i.e. the presence of intrinsic defects; (iii) the presence of impurities, i.e. extrinsic defects; (iv) the size and shape of the particles [33]; (v) the hydroxyl groups concentration.

4. Conclusions

The oxidation of SnO to SnO₂ is strongly depends on the preparation method, the initial oxygen content, and the annealing temperature. The oxidation is started with internal disproportionation and evolved through direct/indirect transformation. During the indirect phase transformation, intermediate phases were involved and the distorted o-SnO phase was also observed. On the other hand, in the case of direct transformation, when SnO comprised a tin matrix similar to the SnO₂ plane it can be easily transformed into SnO₂ with preferred orientation along the axis similar in the atomic distance of the tin matrix.

Optical properties of SnO_x were investigated in UV, VIS, and IR ranges. It was found that the optical bandgap lies between 3.58 and 3.72 eV. The IR transmission of SnO_x, n-type semiconductor, is sharply decreased by electron absorption and the quality of vibrational information concerning form the surface species depends strongly on the nature of the treatment.

References

- [1] T.J. Coutts, X. Liand, T.A. Cessert, IEEE Electron. Lett. 26 (1990) 660.
- [2] G. Martinelli, M.C. Carotta, Sensors Actuators B 15 (1993) 363.
- [3] B. Stjerna, E. Olsson, C.G. Granqvist, J. Appl. Phys. 76 (1994) 3797.
- [4] J.C. Manificier, J.P. Fillard, Thin Solid Films 77 (1981) 67.
- [5] A. Czaplá, E. Kusior, M. Bucko, Thin Solid Films 182 (1989) 15.
- [6] D. Das, R. Banerjee, Thin Solid Films 147 (1981) 321.
- [7] S. Shanthi, C. Subramaniam, P. Ramasamy, Mater. Sci. Eng. B 57 (1999) 127.
- [8] A.E. Rakshani, Y.H.A. Makdisi, Ramazanyan, J. Appl. Phys. 83 (1998) 1049.
- [9] B. Orel, D. Lavrencic- Stanger, K. Kalcher, J. Electrochem. Soc. 141L (1994) 127.
- [10] P. Olive, E.C. Pereira, E. Longo, J.A. Varela, L.O. de, S. Buthoes, J. Electrochem. Soc. 140L (1993) 81.
- [11] J. Isidorsson, C.G. Granqvist, Solar Energy Mater. Solar Cells 44 (1996) 375.
- [12] R.W.G. Wyckhoff, 2nd edn, Co, stal Structures, vol. 1, Wiley, New York, 1963 p. 757.
- [13] M.H.M. Reddy, S.R. Jawalekar, A.N. Chandorkar, Thin Solid Films 169 (1989) 117.
- [14] J. Geurts, S. Rau, W. Richter, F.J. Schmitte, Thin Solid Fibns 121 (1984) 217.
- [15] S. Munnix, M. Schemeits, Phys. Rev. B 33 (1986) 4136.
- [16] P.M.A. Sherwood, Phys. Rev. B 41 (1990) 1051.
- [17] J.-M. Themlin, M. Chraib, L. Henrard, P. Lambin, J. Darville, J.-M. Gilles, Phys. Rev. B 46 (1992) 2460.
- [18] R. Sanjinés, C. Cotuzza, D. Rosenfeld, F. Gozzo, Ph. Alméras, F. Iavy, G. Margafitondo, J. Appl. Phys. 73 (1993) 3997.
- [19] W.K. Choi, H.-J. Jung, S.K. Koh, J. Vac. Sci. Technol. A 14 (1996) 359.
- [20] J.M. Themlin, R. Sporken, J. Darville, R. Claudano, J.M. Gilles, Phys. Rev. B 42 (1990) 11914.
- [21] D.F. Cox, T.B. Fryberger, S. Semancik, Phys. Rev. B 38 (1988) 2072.

- [22] L. Sangaletti, L.E. Depero, B. Allieri, F. Pioselli, E. Comini, G. Sberveglieri, M. Zocchi, *J. Mater. Res.* 13 (1998) 2457.
- [23] A. Diéguez, A.R. Rodríguez, J.R. Morante, P. Nelli, L. Sangaletti, G.J. Sberveglieri, *J. Electrochem. Soc.* 146 (1999) 3527.
- [24] J. Geuets, S. Rau, W. Richter, F.J. Schmitte, *ibid* 121 (1984) 217.
- [25] A.E. Rakshani, Y.H.A. Makdisi, Ramazanyan, *J. Appl. Phys.* 83 (1998) 1049.
- [26] S. Munnix, M. Schmeits, *Phys. Rev. B* 27 (1983) 7624.
- [27] E.W. Thornton, P.G. Harrison, *J. Chem. Soc., Faraday Trans.* 71 (1975) 461.
- [28] P.G. Harrison, A. Guest, *J. Chem. Soc., Faraday Trans.* 85 (1989) 1897.
- [29] G. Centi, F. Trifiro, *Catal. Rev.* 28 (1986) 165.
- [30] D. Amalric-Popescu, F. Bozon-Verduraz, *Catal. Lett.* 64 (2000) 125.
- [31] J. Donaldson, M.J. Fuller, *J. Inorg. Nucl. Chem.* 30 (1968) 1083.
- [32] P. Hollins, *Surf. Sci. Rep.* 16 (1992) 51.
- [33] M. Ocana, V. Fornès, J.V. Garcia Ramos, C.J. Serna, *J. Solid State Chem.* 75 (1988) 364.